



Quenching of reactive species by Avenanthramides: theoretical insight to the thermodynamics of electron transfer

P. C. Sumayya¹ · K. Muraleedharan¹

Received: 31 December 2023 / Accepted: 26 March 2024 / Published online: 13 April 2024

© The Author(s), under exclusive licence to Springer-Verlag GmbH Germany, part of Springer Nature 2024

Abstract

Avenanthramides (AVs) are the phytochemicals found in cereals exclusively in oats. These are widely known natural substances that have antioxidant properties. The free radical deactivation potential of the eight AVs against five reactive species has been studied in physiological pH. At physiological pH, the radical quenching processes were studied using the sequential proton loss followed by electron transfer (SPLET) from the phenolic hydroxyl groups. Using density functional theory (DFT) computations, theoretical studies have been carried out in the gas phase and aqueous solution at M06-2X/6-31 + G (d,p) level of theory. The free radical scavenging ability of the studied AVs was analyzed by using conceptual density functional theory-based parameters and electrostatic potential analysis. By examining the hydrogen atom and electron affinities of each reactive species, the relative destructive potential of each has been compared. The electron transfer capabilities between the studied compound and reactive species were identified by utilizing the ionization energy and electron affinity plots. Additionally, by calculating the redox potentials and equilibrium constants for the entire process in the aqueous solution, the viability of scavenging the free radical species by selected AVs (both in neutral and mono-deprotonated) has been investigated. From the analysis, the neutral as well as the mono-deprotonated form of AVs are found to scavenge $\bullet\text{OH}$ and $\bullet\text{OOH}$, and $\bullet\text{NO}_2$ radicals effectively, while they are inefficient toward the $\text{O}_2\bullet^-$ and $\bullet\text{NO}$ radicals.

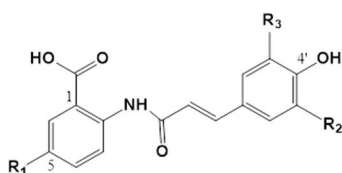
✉ K. Muraleedharan
kmuralika@gmail.com

¹ Department of Chemistry, University of Calicut,
Malappuram 673635, India

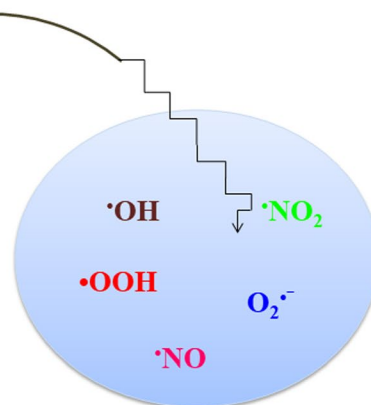
Graphical Abstract



Avenanthramides
(**2p**, **2f**, **2c**, **2s**, **1p**, **1f**,
1c, **1s**)



2p	R1 = OH, R2 = H, R3 = H
2f	R1 = OH, R2 = OCH3, R3 = H
2c	R1 = OH, R2 = OH, R3 = H
2s	R1 = OH, R2 = OCH3, R3 = OCH3
1p	R1 = H, R2 = H, R3 = H
1f	R1 = H, R2 = OCH3, R3 = H
1c	R1 = H, R2 = OH, R3 = H
1s	R1 = H, R2 = OCH3, R3 = OCH3



Scavenging of reactive species

- ✓ HAA & EA
- ✓ IE & EA
- ✓ Redox potential
- ✓ Equilibrium constant

Keywords Avenanthramide · Redox potential · Equilibrium constant · Free radical quenching · Hydrogen atom affinity

1 Introduction

Natural phytochemicals are regarded as a promising source of novel biologically active agents and interesting molecules for the creation of both natural and semi-synthetic medications [1–3]. Their antioxidant activity is the most common and well-documented. Many natural polyphenols, including phenolic acids [4–8], catechins [9], flavonoids [10], anthocyanins [11–13], coumarin [14], stilbenes [15], and terpenes [16], have been shown for intriguing radical scavenging action in vivo and in vitro. Likewise, oats, a grain of the Poaceae family, are one of the staple food crops that human beings can consume directly. Oats stick out as a notable reservoir of polyphenols, including the compound Avenanthramides (AVs) [17, 18]. Among cereals, oats hold a distinctive position as the primary source of these recognized compounds [19, 20], and they exhibit a wide range of biological activities including antioxidant, anti-inflammatory, anti-itch, anti-irritant, and antiatherogenic properties [17–19]. AVs have been reported to exhibit antioxidant activity, with many studies comprising **2p**, **2f**, and **2c** in their experimental analysis using various assays. It was found that **2c** dispenses comparable antioxidant activity to the standard

synthetic antioxidant BHT in the β -carotene test and is more active than Trolox in the DPPH assay [20]. According to the laboratory investigation of antioxidant activity, the activity order is likewise claimed to be $c \geq s \geq f \geq p$, and $2 \geq 1$ [21–24]. From a theoretical point of view, the radical scavenging activity and the underlying mechanisms (HAT, SET, SET-PT, and SLPET) have been documented in our prior research [25] as well as in other studies [26, 27]. However, these earlier investigations enriched our knowledge and opened new space to extend to a little bit more about the radical quenching by these compounds.

Even though free radical production is crucial to the normal functioning of metabolic systems such as cell communication, tissue homeostasis, redox regulation, immunity, defense against infectious illnesses, and many others, their overproduction causes oxidative stress, which leads to cell death, and tissue damage leads to neurodegenerative diseases, cancer, diabetes, and cardiovascular disease [28–30]. The major role of these was taken by the reactive oxygen species (ROS) and reactive nitrogen species (RNS). ROS are produced as a result of regular metabolic processes or in reaction to outside influences like UV radiation. The literature references reactive oxygen and nitrogen species

(RONs) for their recognized harm to biological systems, primarily consisting of superoxide radical anions, hydroxyl, and hydroperoxyl radicals, as well as nitrogen monoxide and nitrogen dioxide radicals, collectively forming ROS and RNS, respectively. The most oxidizing ROS is the hydroxyl radical, which is responsible for DNA oxidative damage. The hydroperoxyl radical's lengthy half-life permits it to reach distant cellular sites. Even though the free radical potential of the nitric oxide radical is minimal, excessive synthesis may cause damage to cells. It may react with the superoxide radical anion to form peroxyxynitrite, a potent oxidizing, and nitrating agent capable of causing protein, lipid, and DNA damage [31].

Although our previous work established the antioxidant activity of these compounds by three basic mechanisms, namely hydrogen atom transfer mechanism (HAT), single electron transfer followed by proton transfer mechanism (SET-PT), and sequential proton loss electron transfer mechanism (SPLET) in the gas phase and ethanol solvents [25], further investigation is required to fully uncover the feasibility of quenching reactive species by the compounds in aqueous solution at physiological pH levels.

Herein, the study extended to the feasibility of radical quenching with five reactive radical species (hydroxyl, hydroperoxyl radicals, superoxide radical anions, nitrogen monoxide, and nitrogen dioxide radicals). For this purpose, the one-electron transfer between the compound and free radical species was analyzed using redox potential and equilibrium constant. Moreover, the results are compared with the hydrogen atom affinity results to ascertain the relative free radical potential of the considered RONs. The radical quenching processes were explained both in the gas phase and the aqueous phase. The study also included a detailed surface analysis electronic structure calculation, and chemical reactivity descriptor investigation to further unravel the intrinsic properties of the compounds. Figure 1 represents the compounds included in the study.

2 Computational details

The calculations were performed, and the geometries of all the structures were fully optimized with M06-2X/6-31 + G (d, p) level of theory using the Gaussian 16W suite [32]. The

optimized structures are given in Fig. S1. A detailed description of conformational search and geometry optimization is given in our previous work [25]. At the same level of theory, the selected free radical species were optimized using the unrestricted open-shell technique. The integral equation formalism of the polarized continuum model (IEF-PCM) was used to account for solvent effects [33]. The solvent water ($\epsilon = 78.35$) was selected to model the aqueous environment. The analyses such as electrostatic potential and chemical reactivity descriptors were finished by Multiwfn 3.8 [34], which is a multifunctional wave function analysis program. The wavefunction files for the compounds were acquired from the Gaussian 16W, which is the input file used by the wavefunction analyzer program Multiwfn 3.8. All isosurface maps were rendered by the VMD 1.9.1 program [35] based on the outputs of Multiwfn. To obtain more accurate results, the grid spacing for the quantitative analyses of the electrostatic potential on the van der Waals (vdW) surface was set to 0.25 Bohr, which is slightly finer than the default settings. The polarizable continuum model was used to include solvent effects. The antioxidant activity results of all the studied compounds obtained from M06-2X/6-31 + G (d, p) methodology are compared with M06-2X/6-311 + + G (d, p) level of theory in aqueous solution.

3 Results and discussion

3.1 Reactivity site analysis

3.1.1 ESP

Herein, to unravel the chemical reactivity of the compounds, the electrostatic potential (ESP) map was utilized for identifying the sites of electrophilic and nucleophilic attack [36]. The electrostatic potential on a van der Waals (vdW) surface of compounds is shown in Fig. 2. The blue regions indicate positive potential, i.e., the sites for nucleophilic attack, while the red regions are prone to electrophilic attack. The green regions are neutral. It can be seen that the blue regions in all the compounds are located on the hydroxyl proton, whereas the red regions lie at the oxygen atoms. Apart from the surface color, the diagrams also represented the quantitative nature of surface local minima (small blue spheres) and

Fig. 1 Chemical structures of selected AVs, and atom labeling are also included (**p**=p-coumaric acid, **f**=ferulic acid, **c**=caffeic acid, and **s**=sinapic acid)[25]

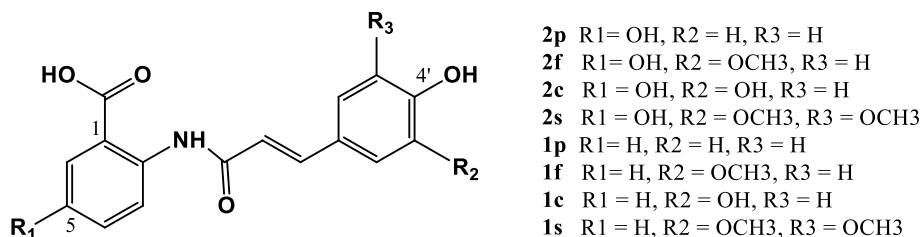
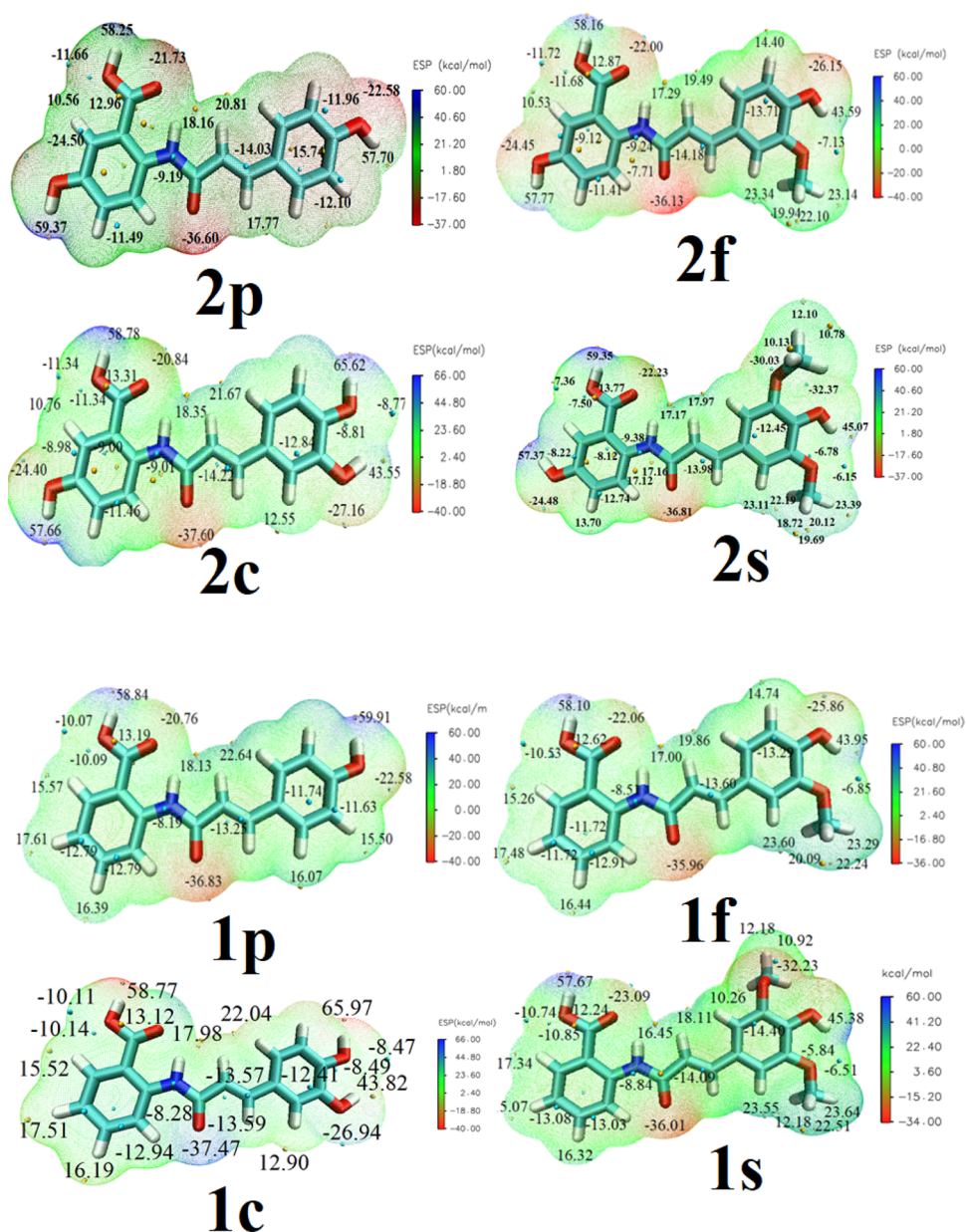


Fig. 2 ESP-mapped molecular vdW surface of the AVs studied. All values are given in kcal/mol



maxima (small orange spheres). The largest negative value was found to be at O9' (carbonyl) in all the compounds, and it lies around 35–37 kcal/mol, which corresponds to the global minimum on the surface. The highest negative potential at the O9' reveals the high delocalizing nature of the carbonyl bond.

For **2p**, the positive potential at 5-OH (59.37 kcal/mol) exceeds that of the acidic protons (58.25 kcal/mol). Conversely, when compared to the 5-OH, the phenolic hydroxyl group at the 4' position exhibits lower positive potential values and is less susceptible to nucleophilic attack. Regarding **1p**, this returns to the same, the 4'OH group is more susceptible to nucleophilic attack. Compared to **2p**, the compound **2f** exhibits lower nucleophilic

attack by the phenolic hydroxylic groups. The positive potential of 4'OH diminishes to 43.59 kcal/mol compared to **2p** which will be due to intramolecular stabilizing interaction with the oxygen of OCH₃. Moreover, for **2c** and **1c**, the highest positive potential or global maximum was found to be arising from the 4' hydroxyl proton (65.62 kcal/mol for **2p** and 65.97 kcal/mol for **1c**). This gives information regarding the intramolecular interactions which are likely to be displayed by the molecule. Also found that substitution of the ortho-position of 4'OH decreases the positive potential value of upon methoxy group (**2s** and **1s**), whereas increases with the hydroxyl group (**2c** and **1c**).

3.1.2 Chemical descriptors

The conceptual density functional theory (CDFT)-based chemical reactivity descriptors such as electronegativity (χ), chemical hardness (η), chemical softness (S), electrophilicity index (ω), and chemical potential (μ) were defined to get a deeper understanding of the chemical reactivity of the compound [37–40] (Eqs. (1)–(8)). The chemical reactivity descriptors are tabulated in Table 1 and calculated using the energy vertical method. The capability of the compound to accept precisely one electron from a donor is measured by its electron affinity (EA), and the measure of the compound to give away an electron is given by its ionization potential (IP) (Eq. (1)–(2)).

$$\text{Vertical ionization potential (VIP)} = E_{\text{cation}} - E_{\text{neutral}} \quad (1)$$

$$\text{Vertical electron affinity (VEA)} = E_{\text{neutral}} - E_{\text{anion}} \quad (2)$$

$$\text{Mulliken electronegativity}(\chi) = \frac{1}{2}(\text{VIP} + \text{VEA}) \quad (3)$$

$$\text{Chemical potential}(\mu) = -\chi \quad (4)$$

$$\text{Hardness}(\eta) = \frac{1}{2}(\text{VIP} - \text{VEA}) \quad (5)$$

$$\text{Softness}(s) = \frac{1}{2\eta} \quad (6)$$

$$\text{Electrophilicity index}(\omega) = \frac{\mu^2}{2\eta} \quad (7)$$

$$\text{Nucleophilicity index}(N_{\text{Avenanthramide}}) = E_{\text{HOMO(Avenanthramide)}} - E_{\text{HOMO(Tetracyanoethylene)}} \quad (8)$$

The chemical hardness of the molecule is the rigidity of the molecule, i.e., the resistance of a molecule to undergo polarization of the atom according to the external environment [38]. It reveals the overall charge cloud and the stability of the molecule. Chemical softness is the reverse of hardness, i.e., it explains the easiness of the electron cloud to undergo polarization [38]. The chemical potential of the molecule is generally the tendency of the electron to move from the region of higher potential to lower potential until it becomes equilibrated. In DFT, chemical potential measures the escaping tendency of an electron from equilibrium and is the negative of electronegativity [41]. Electronegativity is the tendency to attract electrons toward it. The electrophilicity index is the strength of the electrophilicity of the species which is an indication of chemical reactivity and a useful tool in accessing chemical and toxicological potentials of the molecule [40].

The obtained ionization potential and electron affinity are in the range of 7.55–7.87 eV and 0.55–0.60 eV, respectively. These values are comparable to the values of quercetin which is a well-known antioxidant molecule, where IP and EA, respectively, are 7.86 and 1.03 eV. The investigated compound's high ionization potential and low electron affinity demonstrate that it is more difficult to remove an electron than to accept one. The electronegativity of the studied compounds is low compared to quercetin. Hence, the chances of electron transfer from the compounds to neutralize free radical species are high. Similarly, the chemical potential values are also lower than the reference compounds. The chemical potential and electronegativity are the properties of the entire molecule, which remains constant throughout the system. Hardness is identified as the charge density, which is the ability to hold an electronic charge once it has been acquired. Hardness indicates a molecule's difficulty to using electrons, while softness is the inverse of hardness. These characteristics have comparable values to quercetin, indicating their potential as anti-oxidants. The chemical reactivity

Table 1 Chemical reactivity descriptors of the selected AVs obtained at the M06-2X/6–31 + G (d,p) level of theory in the gas phase (Unit eV and for softness eV⁻¹). All the descriptors are calculated for Quercetin and taken as a reference for comparing results

	2p	2f	2c	2 s	1p	1f	1c	1 s	Quer*
IP	7.67	7.55	7.66	7.55	7.93	7.71	7.87	7.68	7.86
EA	0.54	0.55	0.55	0.59	0.59	0.58	0.59	0.60	1.03
Electronegativity	4.11	4.05	4.10	4.07	4.26	4.14	4.23	4.14	4.44
Chemical potential	−4.11	−4.05	−4.10	−4.07	−4.26	−4.14	−4.23	−4.14	−4.44
Hardness	3.57	3.50	3.56	3.48	3.67	3.56	3.64	3.54	3.41
Softness	0.14	0.14	0.14	0.14	0.14	0.14	0.14	0.14	0.15
Electrophilicity index	1.18	1.17	1.18	1.19	1.24	1.21	1.23	1.21	2.89
Nucleophilicity index	2.04	2.16	2.06	2.14	1.82	2.05	1.90	2.03	1.80

* The nucleophilicity index was calculated for tetracyanoethylene

*Quer is quercetin used as a reference to compare results

descriptors of the quercetin were calculated by optimizing the structure with a suitable level of theory.

3.1.3 Gas phase basicity (GPB) and acidity constant (pKa) determination

Next, the order of deprotonation tendencies of each hydroxyl group in the selected AVs was analyzed. The phenolic hydroxyl groups as well as the carboxylic functional group may dissociate or get ionized depending on the pH of the medium. Hence, the step-wise proton release in aqueous solution of compounds was studied by calculating the pKa values of each OH proton using the thermodynamic cycle given in Fig. 3. The gas phase basicity (GPB) was computed as the negative of the Gibbs energy change associated with its protonation reaction in the gas phase.

Applying the thermodynamic cycle given in Fig. 3, the basicity of AV in an aqueous solution was calculated using Eq. (9), and Eq. (10) is used to calculate the pKa values of each deprotonation.

$$\Delta G_{deprot}^0(aq) = GPB + \Delta G_{solv}^0(AV(OH)_{n-1}O^-) + \Delta G_{solv}^0(H^+) - \Delta G_{solv}^0(AV(OH)_n) \quad (9)$$

where $\Delta G_{solv}^0(AV(OH)_n)$ and $\Delta G_{solv}^0(AV(OH)_{n-1})$ are the solvation energies of the AV and its anion, respectively. The standard hydration Gibbs energy of the proton, $\Delta G_{solv}^0(H^+)$, was taken as -265.89 kcal/mol at 298.15 K temperature and 1 atm pressure [42, 43].

$$pK_a = \frac{\Delta G_{deprot}^0(aq)}{RT \ln 10} \quad (10)$$

The computed gas and aqueous solution basicities for the ionization of each hydroxyl group present in the compounds, along with their sequential pKa values, are given in Table 2. The lower pKa value of the carboxylic hydroxyl group of all the selected compounds revealed the predominance of carboxylates of AVs in physiological pH. The previous

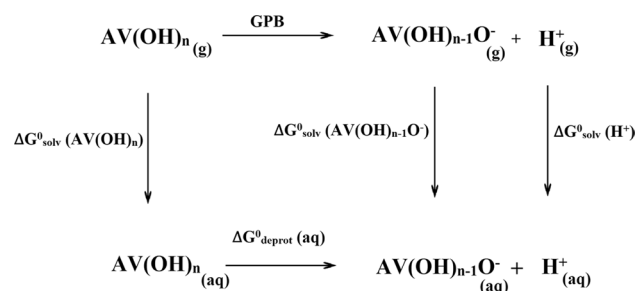


Fig. 3 Thermodynamic cycle to calculate the GPB and pKa values of the deprotonation sites present in AVs (the compound AV is represented as AV(OH)_n for explaining the concepts)

Table 2 Calculated gas and aqueous solution basicities (kcal/mol) and pKa values of AVs

Compound	Bond	GPB	ΔG^0 deprot(aq)	pKa1	pKa2
2p	COOH	317.33	3.36	2.47	–
	5 OH	332.25	18.08	13.31	17.17
	4' OH	323.02	15.97	11.75	12.75
2f	COOH	317.27	4.22	3.10	–
	5 OH	330.21	18.32	13.48	17.76
	4' OH	327.81	18.23	13.42	15.63
2c	COOH	316.16	4.18	3.08	–
	5 OH	331.55	18.30	13.47	17.70
	4' OH	316.18	11.70	8.61	9.92
	3' OH	335.98	20.08	14.78	17.16
2s	COOH	316.30	6.34	4.66	–
	4' OH	325.09	17.04	12.54	13.90
	5 OH	330.72	18.29	13.46	17.21
1p	COOH	317.20	5.82	4.28	–
	4' OH	322.31	15.61	11.49	12.67
1f	COOH	317.55	5.51	4.06	–
	4' OH	327.16	17.60	12.95	14.37
1c	COOH	316.77	4.54	3.34	–
	4' OH	316.09	12.23	9.00	8.73
	3' OH	335.87	21.05	15.49	16.08
1s	COOH	318.19	5.57	4.10	–
	4' OH	325.19	16.67	12.27	13.24

reports also suggest that the compounds containing carboxylic functional groups exist in their monoanionic forms at physiological pH [44]. The entire studied compounds exist in their mono-deprotonated form in biological conditions.

The second deprotonation sites in all the compounds are found to be favored from 4'OH. It refers to the enhanced charge delocalization of anionic species generated from the para-phenolic group via extended conjugation. On comparing, the pKa for second deprotonation, the lower was found to be for caffeic acid derivatives, **2c** and **1c**, 9.92 and 8.73 kcal/mol, respectively. The lower value of pKa of **2c** and **1c** will be due to stabilization by intramolecular hydrogen bonding from the nearest hydroxyl group in addition to the charge delocalization. The obtained pKa values are consistent with the experimentally reported pKa values of the caffeic acid [45, 46]. Literature reports the pKa values of the acidic proton, 4'OH, and 3'OH, respectively, 3.6–4.49, 8.6–9.3, and 10.3–12.7 kcal/mol [45, 46]. The methoxy substitution (electron-donating) ortho to 4' OH decreases the tendency of proton transfer due to the formation increased charge cloud near the anionic species. For **2c** and **1c**, the pKa values 5 OH and 3'OH lie in the range of 16–18, meant for the higher basicity. The bulkiness and type of the substituents are two significant elements that influence the deprotonation sequence. Furthermore, the stability of the

resultant anionic species is important in defining the subsequent deprotonation and pKa values of the phenolic groups.

The pKa values show that the compounds exist as their mono-deprotonated forms (carboxylate form) at physiological pH. With the increase in pH, the next deprotonation occurs from the 4'-OH phenolic hydroxyl group of the compounds which results in the formation of dianion of AV. The pH range at which each compound forms its dianion changes according to the structure. The compound **1c** and **2c** around pH 8.7 and 9.92, respectively, forms their AV 4'-O-monoanion carboxylates. The pKa values of other AVs **2p**, **2f**, **2s**, **1p**, **1f**, and **1s**, respectively, for the formation of its di-anionic form are 12.75, 15.63, 13.9, 12.67, 14.37, and 13.24. It means that these compounds form 4'-O⁻ anion from the carboxylate forms of its corresponding AV at an increased pH value. Figure 4 represents the effect of pH on the ionization of **2c**.

3.2 Radical scavenging activity

Our previous study reported the antioxidant activity of the compound by HAT, SET-PT, and SPLET mechanisms in the gas phase and ethanol medium [25]. Our study concluded the preference HAT mechanism in the gas phase and the SPLET mechanism in the ethanol medium [25]. In the HAT mechanism, the radical deactivation occurs through the donation of hydrogen atoms by the phenolic OH groups in each compound, and also obtained that the carboxylic acid proton and amide proton (N-H) are least stable for the radical quenching process. In the solution phase, phenolic OH groups scavenge free radical species by forming its anion and followed by electron transfer. (COOH and N-H proton are obtained to be less significant due to comparatively higher value of ETE.) Later on, Xue et al. [26]. and Purushothaman and co-workers [27] concluded expression of the same mechanism in both gas phase and solution phases. The HAT, SET-PT, and SPLET parameters and a detailed description of these mechanisms of the AVs in aqueous solution are

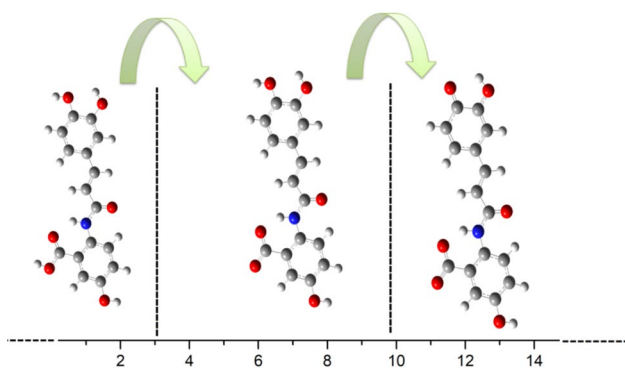


Fig. 4 Effect of pH on the ionization of **2c**

explained in the supplementary information (Section S1 and Table S1, Table S2, Table S4). Herein, we compared the results of antioxidant activity with M06-2X/6-31 + G (d, p) and M06-2X/6-311 + + G (d, p) levels of theories and also the antioxidant activity of phenolic hydroxyl groups in deprotonated form (carboxylate form of each compounds) of each compounds also included.

From Table S1, it can be observed that for the compounds **2p** and **2f**, the lowest BDE is exhibited by the 5-OH followed by 4'-OH, and in other cases, the 4'-OH is followed by 5-OH. No much change in BDE was observed in the aqueous phase. However, it follows the same trend as the gas phase of each molecule under consideration. In the aqueous phase, the BDE value of 4'-OH is found to be lower than in the gas phase due to greater stabilization of the radical formed. The compound **2c** and **1c** possess the lowest BDE among others through 4'-OH with BDE of approximately 77–79 kcal/mol. The lowest energy revealed the stabilization of radicals formed through delocalization through the ring [25] and the stabilization of the radicals formed by intramolecular hydrogen bonds. In the aqueous solution, the BDE of the 4'-OH slightly increased. It may be due stabilization of radicals formed with hydrogen from the solution, which is less feasible than stabilization through delocalization. For 3'-OH and 5-OH, the bond becomes more potent in the aqueous phase by their lower BDE values compared to the gas phase values which will be due to the stabilization of radicals formed through the solvent cage effect. Considering **2f** and **2s**, the presence of a methoxy group ortho to 4'-OH decreased the BDE value of 4'-OH but was still greater than 5-OH, and the addition of second methoxy group, a decrease in BDE much less than 5-OH was observed. So for **2s** hydrogen donation, capability of 4'-OH becomes more favorable than **2f** and **2s** and hence has a higher H-donating ability. So based on the BDE, the hydrogen donating capability obeys the order **2c** > **1c** > **2s** > **1s** > **2f** > **1f** > **2p** > **1p** in the gas phase and aqueous phase. The order obtained is consistent with the order of radical-trapping activity in the DPPH assay [22]. The results of BDE values are very close to each other in both levels of theories and follows the same trends among compounds. The change BDE value of 0.27 kcal/mol is obtained for 4'-OH of **2c** in M06-2X/6-311 + + G (d, p) compared to M06-2X/6-31 + G (d, p). The differences between both levels of theories values are found to be not greater than 10 kcal/mol [7].

The ionization potential (IP) of AVs becomes lesser in the aqueous phase revealing the high electron transferability in the aqueous phase than gas phase (Table S2). The sequence of IP values of compounds in the gas phase is observed to be **2s** < **2f** < **2p** < **2c** < **1s** < **1f** < **1c** < **1p** in the gas phase, whereas in the aqueous phase, it follows **1f** < **2p** < **2s** < **2p** < **1s** < **1c** < **1p** < **2f** < **2c**. The order of radical scavenging activity is much different from the HAT mechanism

because IP value influences the whole structure of the molecule, whereas HAT is affected by the local phenomena induced by the substituents. Even though the IP values in gas phase not much deviates in both theories and follows same trend, an observable deviation is found in aqueous phase, approximately of 23 kcal/mol. But still both theories follows same trend in activity. The higher IP values in M06-2X/6-31 + G (d, p) are found to be due to the very low solvation enthalpies of electron in aqueous phase. Solvation enthalpies of electron and proton in both levels of theories in both solvents are given in Table S3. The solvation enthalpies of electron in aqueous phase both M06-2X/6-311 + + G (d, p) and M06-2X/6-31 + G (d, p) levels of theories are -0.041879 and -0.002978 Hartree, respectively, which are calculated by methodology suggested by Marković et al.[47].

The proton dissociation enthalpy values obtained by the deprotonation of radical cation formed in the aqueous phase are more feasible than the gas phase of approximately 200 kcal/mol. The 4'OH of **1c** and **2c** has the lowest value of PDE in both phases. The 4'OH of each compounds possesses lower PDE value among other OH groups in the respective molecules except for **2p** and **2f**. For **2p** and **2f**, the 5OH has lower PDE value. The PDE values of each compounds differ only approximately of 1 kcal/mol with M06-2X/6-311 + + G (d, p) and M06-2X/6-31 + G (d, p) levels of theories, and both follows same trend. The lower PDE value in aqueous phase than the BDE value does not conclude the feasibility of the mechanism toward radical scavenging activity. Because, to reach the second step, (i.e., PDE), the compounds should overcome the energy barrier of first step (IP). So when compared to BDE values, IP values are very high. Hence, SET-PT mechanism can be excluded from the antioxidant activity of selected compounds in aqueous phase too.

The parameters of SPLET mechanism in aqueous phase, the PA, and ETE value both M06-2X/6-311 + + G (d, p) and M06-2X/6-31 + G (d, p) levels of theories are given in Table S4. As expected, PA values in the aqueous medium are lower than the gas phase and also lower than the BDE value corresponding in the aqueous medium. Hence in polar solvent, herein in water, the AVs favor deprotonation of the hydroxyl group. The PA values are very close in both the level of theories, and the differences in enthalpies are less than one kcal/mol. In aqueous medium, the PA values are around 280 kcal/mol lower than the gas phase. Among the selected compounds, the c-series compounds (**2c** and **1c**) possess lower PA values and which is by the group 4'OH. The second step of SPLET mechanism is the electron movement from the anionic form of the compound. The ETE is the corresponding descriptor. Due to low solvation enthalpy value of electron, the ETE value calculated using M06-2X/6-311 + + G (d, p) are found to be lower than M06-2X/6-31 + G (d, p) as explained in

case of IP values. The difference is around 20–24 kcal/mol. Hence, the M06-2X/6-311 + + G (d, p) level of theory is better for explaining the SPLET mechanism in aqueous phase. Both the results of M06-2X/6-31 + G (d, p) and M06-2X/6-311 + + G (d, p) follow same trend in reactivity.

Considering PA + ETE values, the 4'-OH of **2c**, **2s**, **1p**, **1f**, **1c**, and **1s** are found to be less energy demanding toward radical scavenging mechanism. For **2p** and **2f**, the 5-OH is found to be more reactive due to its comparatively lower energy. These are the active groups in the selected compounds, where the SPLET process is most likely to occur in polar liquids. The order of radical scavenging ability in polar solvent follows as **2c** > **1c** > **2s** > **1s** > **2f** > **1f** > **2p** > **1p**. The order was in good agreement with the experimental results [22]. The order is consistent with that of the HAT mechanism. Considering **2** series compounds, the PA values of 5-OH do not change appreciably upon changing the substitution on the B-ring which means that substitution on the B-ring does not affect the A ring. Moving from **2f** to **2c** and **2s**, the deprotonation from the B-ring becomes more feasible due to the stabilization of the ortho-substituent. The ETE values are very close to each other, indicating that the introduction of substituent on the B-ring has a minor effect on the electron-donating ability of 5-O⁻ anionic forms. Moreover, as given **2** series and **1** series compound, the OH substituent on the 5th position has little effect on the B-ring.

Hence in an aqueous solution, the SPLET pathway is the preferred mechanism, in which the OH group first forms its anion and further electron transfer leads to radical deactivation and the compound forms its radical. The generated radical further stabilized through the resonance.

The selected compounds in all cases contain a -COOH functional which gets ionized and forms its carboxylates in solution phase, which is evident from pKa calculations. Hence, the antioxidant activity of carboxylate forms of all compounds is calculated in aqueous phase and tabulated in Table S5. The descriptors BDE, IP, PDE, PA, and ETE values are reported in Table S5. From the descriptors, the PDE values are found to be lower than other descriptors but in higher value of IP, the SET-PT mechanism can be excluded from the explaining antioxidant potential of the compounds as discussed above. The PA values are found to be lower than the BDE values. Hence, SPLET will be the thermodynamically preferred pathway in carboxylate form of compounds also. The lowest PA value is exhibited by the **2c** by the 4'-OH group followed by **1c** by the same group. These values are found to be slightly higher than the non-dissociated or unionized form of the compound (**2c** in non-dissociated form PA = 45.58 kcal/mol, **2c** carboxylate form PA = 46.87 kcal/mol). The order of PA + ETE follows as **2c** > **1c** > **2s** > **1s** > **2f** > **1f** > **2p** > **1p**. The order is consistent with the non-dissociated form of compounds.

In conclusion, HAT and SPLET is the thermodynamically preferable mechanism in gas phase and aqueous phase, respectively. The results of the antioxidant descriptors, BDE, PA, and PDE, produces close results with M06-2X/6-311 + +G (d, p) and M06-2X/6-31 + G (d, p) methodologies, and deviations were observed with IP and ETE values. It was observed that the large difference in the solvation enthalpies of electron in aqueous media is the reason for deviation. Hence, calculations involving electron solvation enthalpies in water media can be better explained by higher levels of theories, and otherwise, M06-2X/6-31 + G (d, p) was found to be sufficient.

3.2.1 Quenching of reactive oxygen species and nitrogen species (RONs)

Reactive oxygen and nitrogen species (RONs) are vital in cell signaling, immunity, and tissue homeostasis and are required for proper physiological activities [48, 49]. Excess radical species, on the other hand, are implicated in the development and accelerated pathogenesis of a variety of disorders [48]. The common radical species ROS include oxygen-based free radicals, such as the superoxide radical anion ($O_2^{\bullet-}$), hydroxyl (HO^{\bullet}), alkoxy (RO^{\bullet}), organic peroxy (ROO^{\bullet}), and hydroperoxy (HOO^{\bullet}) radicals. RNS comprises peroxy nitrite ($ONOO^-$), nitric oxide (NO^{\bullet}), and nitrogen dioxide (NO_2^{\bullet}) [50]. We considered five RONs that are significant for biological systems among reactive free radicals. The hydroxyl, hydroperoxy radicals, and superoxide radical anions are selected under ROS and nitric oxide and nitrogen dioxide radicals among RNS.

3.2.2 Hydrogen atom affinity (HAA) and electron affinity (EA)

The energy needs of AVs and selected radical species are essential in predicting probable radical scavenging processes. So for this purpose, the hydrogen atom affinity (HAA) and electron affinity (EA) of each radical species were calculated both in the gas phase and aqueous medium with the help of Eqs. (11) and (12), respectively, for HAA and EA.



where R^{\bullet} represents the radical species, R^{-} is the radical after one electron acceptance and RH is the protonated radical species. The triplet state of NO^{\bullet} was considered for calculating the EA. The values of H^{\bullet} and e^{-} were calculated using the method. The frequently recognized value of 0.7530 kcal/mol for the electron enthalpy can be used to calculate the standard values of electron enthalpies in the

gas phase [51]. The enthalpies of hydrogen radicals and electrons in the gas phase and water phase are calculated by the methodology proposed by Marković et al. [47]. The enthalpy values for the hydrogen atom and electron are tabulated in Table S3 both in gas phase and aqueous phase using M06-2X/6-311 + +G (d, p) and M06-2X/6-31 + G (d, p) levels of theories.

The computed HAA and EA values are tabulated in Table 3. The highest HAA value of hydroxyl radical among all radicals in the gas phase and aqueous phase describes the highly destructive nature of the OH radical. The $O_2^{\bullet-}$ and NO^{\bullet} radicals are in the lower range, suggesting that they are fruitless at accepting a hydrogen atom either in the gas phase or in an aqueous solution. Further, the HAA of the majority of the species under examination increases upon solvation. The HAA values calculated both in gas phase and aqueous phase are very close with two levels of theories and hence both are acceptable.

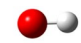
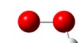
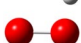
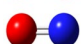
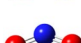



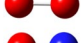

The tendency of electron acceptance and formation of its anion is higher for NO_2^{\bullet} followed by OH^{\bullet} and OOH^{\bullet} in the gas phase. The electron acceptance and formation of corresponding anion O_2^{2-} is found to be quite energetically unfavorable in the gas phase due to its positive electron affinity but favorable upon solvation. The negative value of NO^{\bullet} radical in the gas phase is also meant for the lower free radical potential. However, the EA values of each reactive species are found to be much higher in the solution phase as compared to the gas phase. The EA values in aqueous solution with M06-2X/6-311 + +G (d, p) are found to be much lower than M06-2X/6-31 + G (d, p) methodologies, which will be due to the very low solvation enthalpy of electron in aqueous phase in M06-2X/6-31 + G (d, p) method (Table S3). The trends in activity concluded are same in both methodologies.

In conclusion, according to HAA and EA values, hydrogen atom acceptance and detoxification through the HAT (hydrogen atom transfer) mechanism will be highly favorable for the radicals, hydroxyl, hydroperoxy, and nitrogen dioxide radicals among selected free radical species in the gas phase and aqueous phase. The SET or SET-PT mechanism, which includes the transfer of a single electron (connected with EA value in Table 3), is unfavorable for superoxide radical anions and nitric oxide in the gas phase, and it is higher for radicals OH^{\bullet} , OOH^{\bullet} , and NO_2^{\bullet} in both solutions. In the SPLET mechanism, the second step is electron acceptance (by radical species from antioxidant species) also favorable for OH^{\bullet} , OOH^{\bullet} , and NO_2^{\bullet} radicals due to their feasible EA values.

3.2.3 Electron Affinity (EA) versus Ionization Energy (IE) map

To assess the electron transfer power between the radical and the selected compounds, vertical ionization energy

Table 3 Computed HAA and EA of the considered ROS/RNS (kcal/mol) in the gas phase and aqueous solution both in M06-2X/6-31+G (d, p) and M06-2X/6-311++G (d, p)

	RONS	HAA		EA	
		Gas	Aqueous	Gas	Aqueous
M06-2X/6-31+G (d, p)	$\cdot\text{OH}$ 	-116.37	-118.28	-36.55	-114.22
	$\cdot\text{OOH}$ 	-84.98	-85.56	-21.50	-92.30
	$\text{O}_2^{\cdot-}$ 	-59.99	-65.57	165.71	-38.55
	$\cdot\text{NO}$ 	-47.02	-49.50	-5.66	-72.40
	$\cdot\text{NO}_2$ 	-80.27	-83.36	-55.95	-117.71
M06-2X/6-311++G (d, p)	$\cdot\text{OH}$ 	-116.10	-117.88	-37.17	-90.37
	$\cdot\text{OOH}$ 	-85.12	-85.59	-22.80	-69.18
	$\text{O}_2^{\cdot-}$ 	-59.82	-65.30	166.03	-14.52
	$\cdot\text{NO}$ 	-45.98	-48.39	-5.64	-48.10
	$\cdot\text{NO}_2$ 	-79.59	-82.41	-56.03	-93.37

(IE) and vertical electron affinity (EA) were employed. It has previously been observed that antioxidant species could either give or take up an electron to scavenge free radicals [52, 53]. This demonstrates that the electron transfer reaction is governed by the ionization energy and the electron affinity of the antioxidant and the free radical. Low ionization energy indicates that the molecule will donate an electron at a low energetic cost, but high electron affinity indicates that the molecule will readily take an extra electron. Here, the single electron transfer tendencies of the compounds are considered.

For this purpose, the IE versus EA map includes selected free radicals, selected AVs, and their mono-deprotonated forms (carboxylates) (Fig. 5 and Table 4). The electron flow will occur from molecules in the bottom left area of the map to molecules in the top right section of the map. Hence, a radical scavenging action will take place. All the AVs and their mono-deprotonated forms lie in the bottom left area of the map and are better electron donors and worse electron acceptors than the $\cdot\text{OH}$, $\cdot\text{OOH}$, and $\cdot\text{NO}_2$ radicals. Hence, they are predicted to act as electron donors to deactivate these free radicals.

Selected AVs and their mono-deprotonated equivalents, as well as the free radicals $\text{O}_2^{\cdot-}$ and $\cdot\text{NO}$, are localized more or less at the same position in the map. As a result, no electron transfer between AVs or mono-deprotonated forms and the radicals $\text{O}_2^{\cdot-}$ and $\cdot\text{NO}$ is expected. As can be seen from Table 4 and Fig. 5, deprotonated forms are better electron donors than the neutral form of the molecule. The electron affinities are lower in mono-deprotonated molecules than the neutral molecules. According to these

results, deprotonated AVs will be better scavengers for radicals $\cdot\text{OH}$, $\cdot\text{OOH}$, and $\cdot\text{NO}_2$ than AVs.

3.2.4 Redox potentials and equilibrium constant calculations of AVs with reactive species

From our previous calculations, it was found that the compounds in the aqueous solution preferred the SPLET pathway (proton dissociation and electron transfer) to scavenge the free radical species. Moreover, Xue and colleagues [26] reported the presence of a monoanionic form of the AVs at physiological pH and also confirmed from previous pKa calculations (formation of carboxylates at low pH). Thus, we have considered the viability of various reactive species under study by AVs through a SPLET pathway in the aqueous solution at physiological pH. The redox potential and equilibrium constant for the overall reaction were calculated by employing the previously reported methodologies [54]. Let us now explore if neutral and mono-deprotonated versions of compounds in an aqueous solution could effectively scavenge various RONS. The overall redox reaction of neutral and mono-deprotonated AV with RONS can be represented by Eqs. (13) and (14), respectively. In Eq. 13, the overall route of radical deactivation by the neutral form of the compound (non-dissociated) of AV through the SPLET pathway is included, whereas in Eq. 14, the mono-deprotonated form or carboxylate form of AVs is considered. The feasibility of scavenging radicals by the pathway is analyzed by calculating the redox potential and equilibrium constant values.

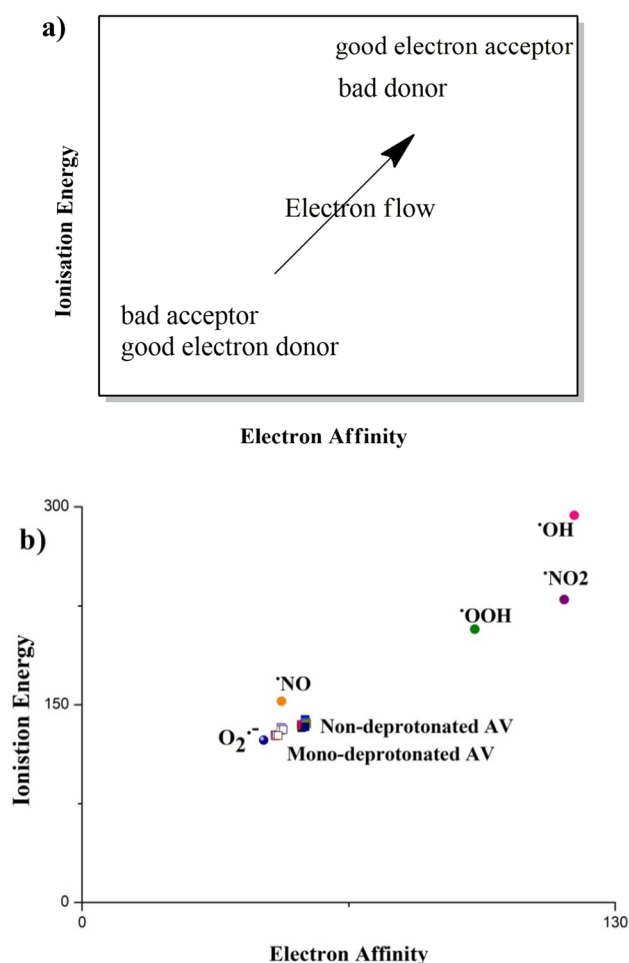
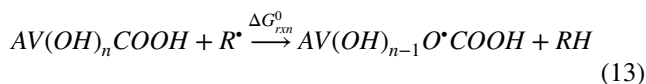


Fig. 5 Map allows a straightforward comparison of the electron donor–acceptor capability of AVs (squares), mono-deprotonated AVs (squares with filled colors), and radicals $\bullet\text{OH}$ (circle-pink), $\bullet\text{OOH}$ (circle-light green), $\text{O}_2\bullet^-$ (circle-royal blue), $\bullet\text{NO}$ (circle-orange), and $\bullet\text{NO}_2$ (circle-purple) in water (values are given in kcal/mol)



Using the three thermodynamic cycles given in Fig. 6, the redox potential was calculated. The first step of the SPLET mechanism, i.e., loss of a proton (Eq. (15)), and the second step, scavenging of the free radical species (Eq. (16)) are shown as

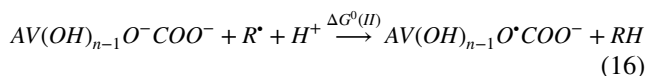
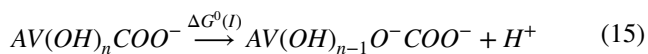


Table 4 Ionization energy and electron affinity value (kcal/mol) of the selected compound, mono-deprotonated species, and radicals using M06-2X/6-31 + G (d, p) level of theory

	Species	Vertical ionization energy	Vertical electron affinity
Radicals	$\bullet\text{OH}$	286.26	116.26
	$\bullet\text{OOH}$	203.36	93.67
	$\text{O}_2\bullet^-$	116.97	39.87
	$\bullet\text{NO}$	146.52	73.47
	$\bullet\text{NO}_2$	230.92	119.06
Non-deprotonated AVSs	2p	135.09	53.41
	2f	132.60	53.52
	2c	134.20	53.70
	2s	133.35	54.31
	1p	138.95	54.36
	1f	134.66	54.37
	1c	136.84	54.58
	1s	135.44	54.80
Mono-deprotonated AVs	2p	127.22	47.07
	2f	126.39	47.15
	2c	127.20	47.36
	2s	126.72	47.82
	1p	132.97	48.45
	1f	130.72	48.40
	1c	132.35	48.64
	1s	131.30	49.01

The reaction (16) may split up into two half-cell reactions represented as (Eqs. (17) & (18))



The standard Gibbs free energy change for the redox reaction (ΔG^0_{rxn}) can be calculated using Eq. (19),

$$\Delta G^0_{\text{rxn}} = \Delta G^0(I) + \Delta G^0(II) \quad (19)$$

where $\Delta G^0(I)$ is the Gibbs energy change for the step of deprotonation (first step) and $\Delta G^0(II)$ for the second step.

$$\begin{aligned} \Delta G^0(I) = & \Delta G^0_{\text{gas}}(I) + \Delta G^0_{\text{solv}}(\text{AV}(\text{OH})_{n-1}\text{O}^-\text{COO}^-) \\ & + \Delta G^0_{\text{solv}}(\text{H}^+) - \Delta G^0_{\text{solv}}(\text{AV}(\text{OH})_n\text{COO}^-) \end{aligned} \quad (20)$$

$$\Delta G^0(II) = \Delta G^0(i) + \Delta G^0(ii) \quad (21)$$

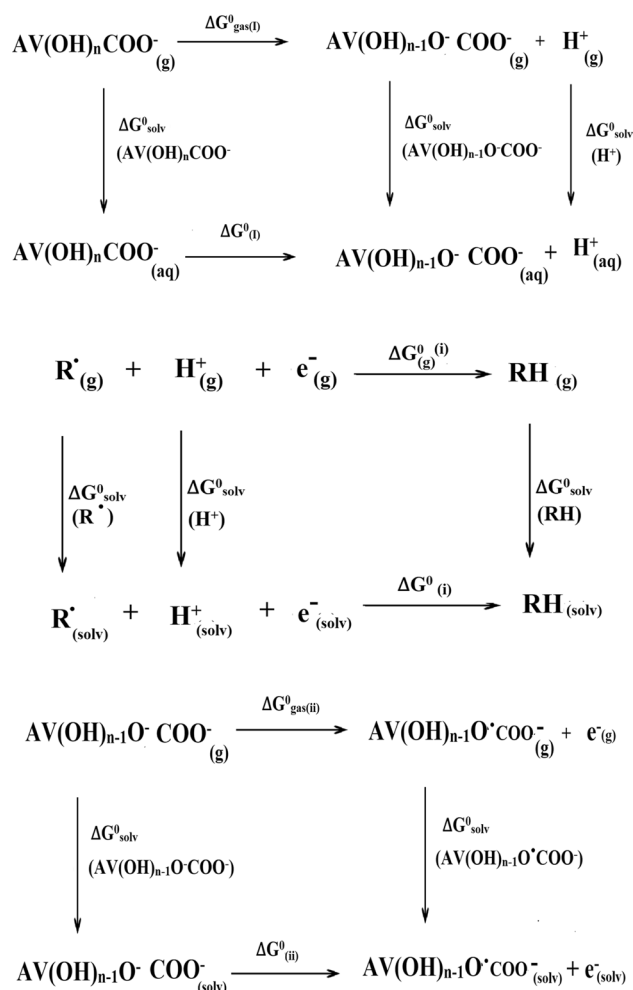


Fig. 6 Thermodynamic cycles to compute the standard Gibbs energy change for different reactions in aqueous solution

$$\Delta G^0(i) = \Delta G^0_{(g)}(i) + \Delta G^0_{\text{solv}}(\text{RH}) - \Delta G^0_{\text{solv}}(\text{R}^{\bullet}) - \Delta G^0_{\text{solv}}(\text{H}^+) \quad (22)$$

$$\Delta G^0(ii) = \Delta G^0_{(g)}(ii) + \Delta G^0_{\text{solv}}(\text{AV(OH)}_{n-1}\text{O}^-\text{COO}^-) - \Delta G^0_{\text{solv}}(\text{AV(OH)}_{n-1}\text{O}^-\text{COO}^-) \quad (23)$$

Then, the corresponding redox potentials and the equilibrium constants were calculated using Eqs. (24) and (25), respectively, with different radical species. Here, F represents the Faraday constant ($23.06 \text{ kcal mol}^{-1} \text{ V}^{-1}$).

$$E_{rxn} = \frac{-\Delta G^0_{rxn}}{F} \quad (24)$$

$$\log K = \frac{FE_{rxn}}{2.303RT} \quad (25)$$

The equilibrium constant and redox potential for the radical reaction are tabulated in Table 5 in

M06-2X/6-31+G(d, p) methodology. From the table, it is observed that among the considered reactive species, the hydroxyl group has the highest value of equilibrium constant and redox potential values for both neutral and mono-deprotonated forms of all compounds. Therefore, we can say that the scavenging of hydroxyl radicals by the compounds at the physiological pH is highly advantageous and spontaneous. The Gibbs free energies corresponding to the scavenging process via the SPLET mechanism are also found to be highly negative for hydroxyl radicals in all cases (both non-deprotonated and deprotonated forms) indicating the feasibility of radical deactivation aqueous solution (Table S6).

Among the species, **c**-series compounds have a higher equilibrium constant than others for all reactive species followed by **s**-series compounds. In **c**-series compounds, **2c** possesses higher radical quenching in the non-dissociated form and **1c** in the mono-deprotonated form. The order of radical scavenging activity follows caffeic acid (**c**-series) > sinapic acid (**s**-series) > ferulic acid (**f**-series) > p-coumaric acid (**p**-series). These results are in line with the previously reported studies on radical scavenging activity [22, 26]. The higher scavenging activity of the **c**-series and **s**-series of compounds was due to the presence of stabilizing hydroxyl and methoxy groups. The equilibrium constant and redox potential of all the compounds including both forms are negative for $\text{O}_2\cdot^-$ and NO radicals. Hence, these radicals are not scavenged by the selected AVs. The $\cdot\text{OOH}$ radicals are scavenged by all the compounds except **1p**. Likewise, NO_2 also exhibits a positive equilibrium constant in most of the cases (**2f** neutral state and **1p** in both forms are exceptions) and shows that it also can scavenge the selected compounds.

The higher values of the equilibrium constants in the case of the mono-deprotonated forms indicate their greater potential for scavenging the reactive species. The ease of scavenging of the considered RONS by both the neutral and mono-deprotonated forms of compounds follows the order: $\cdot\text{OH} > \cdot\text{OOH} > \cdot\text{NO}_2 > \text{O}_2\cdot^- > \cdot\text{NO}$, which is consistent with the order of the hydrogen atom affinity (HAA) in aqueous solution.

4 Conclusions

In the present work, we have explored the feasibility of quenching five free radical species by eight main oat phenolic antioxidant Avenanthramides; **2p**, **2f**, **2c**, **2s**, **1p**, **1f**, **1c**, and **1s** using M06-2X/6-31+G(d, p) as well as M06-2X/6-311+G(d, p) level of theories. Theoretical elucidation of quenching of free radical species by selected

Table 5 Calculated redox potential (E_{rxn}) in V, and the equilibrium constant (K) for the scavenging of each reactive species by the neutral and monoanionic form (bracket) of AVs via the sequential proton loss electron transfer mechanism in M06-2X/6-31+G (d, p) level of theory

RONs	Redox potential (E_{rxn})							
	2p	2f	2c	2 s	1p	1f	1c	1 s
•OH	1.58 (1.50)	1.51 (1.55)	1.70 (1.71)	1.63 (1.66)	1.47 (1.42)	1.54 (1.55)	1.67 (1.77)	1.63 (1.64)
•OOH	0.13 (0.05)	0.06 (0.10)	0.25 (0.26)	0.17 (0.21)	0.02 (-0.03)	0.09 (0.10)	0.22 (0.32)	0.18 (0.18)
$\text{O}_2^{\bullet-}$	-0.67 (-0.75)	-0.74 (-0.70)	-0.55 (-0.54)	-0.62 (-0.59)	-0.78 (-0.83)	-0.71 (-0.70)	-0.58 (-0.48)	-0.62 (-0.61)
•NO	-1.39 (-1.47)	-1.46 (-1.42)	-1.27 (-1.26)	-1.34 (-1.31)	-1.50 (-1.55)	-1.43 (-1.42)	-1.30 (-1.19)	-1.34 (-1.33)
•NO ₂	0.05 (-0.03)	-0.02 (0.02)	0.17 (0.19)	0.10 (0.13)	-0.06 (-0.1)	0.02 (-0.02)	0.14 (0.25)	0.10 (0.11)
	Equilibrium constant (K)							
•OH	6.27×10^{26} (2.77×10^{25})	3.90×10^{25} (1.82×10^{26})	6.10×10^{28} (1.05×10^{29})	3.79×10^{27} (1.33×10^{28})	7.68×10^{24} (1.24×10^{24})	1.35×10^{26} (1.95×10^{26})	2.06×10^{28} (1.21×10^{30})	4.31×10^{27} (5.70×10^{27})
•OOH	1.48×10^2 (6.55)	9.22 (4.32×10^1)	1.45×10^4 (2.48×10^4)	8.97×10^2 (3.16×10^6)	1.82 (2.93×10^{-1})	3.19×10^1 (4.61×10^1)	4.88×10^3 (2.87×10^5)	1.02×10^3 (1.35×10^3)
$\text{O}_2^{\bullet-}$	4.16×10^{-12} (1.83×10^{-13})	2.58×10^{-13} (1.21×10^{-12})	4.05×10^{-10} (6.96×10^{-10})	2.51×10^{-11} (8.85×10^{-11})	5.09×10^{-14} (8.22×10^{-15})	8.95×10^{-13} (1.29×10^{-12})	1.37×10^{-10} (8.04×10^{-9})	2.86×10^{-11} (3.78×10^{-11})
•NO	2.85×10^{-24} (1.26×10^{-25})	1.77×10^{-25} (8.28×10^{-25})	2.77×10^{-22} (4.77×10^{-22})	1.72×10^{-23} (6.06×10^{-23})	3.49×10^{-26} (5.63×10^{-27})	6.13×10^{-25} (8.84×10^{-25})	9.35×10^{-23} (5.51×10^{-21})	1.96×10^{-23} (2.59×10^{-23})
•NO ₂	8.41 (0.37)	5.22×10^{-1} (2.44)	8.19×10^2 (1.41×10^3)	5.08×10^1 (1.79×10^2)	1.03×10^{-1} (1.66×10^{-2})	1.81 (2.61)	2.76×10^2 (1.63×10^4)	5.78×10^1 (7.65×10^1)

variants of compounds is addressed for the first time, even though various theoretical and experimental examinations of the antioxidant activity of these molecules have previously been conducted. The investigation of radical scavenging activity of the selected compounds in an aqueous solution utilizing the mechanism HAT, SET-PT, and SPLET employing the thermochemical parameters like bond dissociation enthalpy, ionization potential, proton dissociation enthalpy, proton affinity, and electron transfer enthalpies signifies the preference of SPLET pathway at the physiological pH. This is also proved by the pKa calculations. We already proved the choice of the HAT mechanism in the gas phase in our previous work. The order of free radical scavenging activity of selected compounds in aqueous solution at the physiological pH is found to be **2c** > **1c** > **2 s** > **1 s** > **2f** > **1f** > **2p** > **1p**. The obtained results are in accordance with the experimental findings.

Among the studied RONs, •OH, •OOH, •NO₂, O₂•⁻, and •NO, using the redox potential and equilibrium constant for one-electron transfer between the Avenanthramides and free radical species, the hydroxyl radical is shown to display the best affinity for hydrogen and electrons. The high equilibrium constants for the hydroxyl radical indicate that it is easily scavenged by AVs at physiological pH levels. We may also conclude that the neutral and mono-deprotonated forms of the AVs are effective at scavenging the hydroxyl and hydroperoxyl radicals as well as the nitrogen dioxide

radical based on the computed equilibrium constant values. The superoxide radical anion and nitrogen monoxide radical are shown to be ineffective by the selected compounds. Among AVs, the free radical quenching of caffeic acid derivatives (**c-series** compounds; **2c** & **1c**) is found to be more reactive followed by sinapic acid derivatives (**s-series** compounds; **2 s** & **1 s**). Compared to **c-series** and **s-series** compounds, **f-series** (**2f** & **1f**) and **p-series** (**2p** & **1p**) compounds are found to be less in radical quenching processes. The results obtained are strictly coinciding with reported experimental antioxidant activity. The ease of scavenging of the considered RONs by both the neutral and mono-deprotonated forms of compounds follows the order: •OH > •OOH > •NO₂ > O₂•⁻ > •NO, which is consistent with the order of the hydrogen atom affinity (HAA) in aqueous solution. The results conclude the higher free radical quenching ability of **c-series** and **s-series** compounds, respectively, due to ortho-dihydroxy and guaiacyl moieties on the aromatic ring, which delivers higher radical stability through internal H bonds, as the superior radical scavenger.

Supplementary Information The online version contains supplementary material available at <https://doi.org/10.1007/s00214-024-03111-2>.

Acknowledgements The author Sumayya P.C. expresses sincere gratitude to UGC-MANF for financial support (Research fellowship). The authors are also thankful to the Central Sophisticated Instrumentation

Facility (CSIF) of the University of Calicut for the Gaussian 16 software support.

Author contributions S.P.C. involved in idea, methods, software, experiment setup, preparation of data and evaluation, and paper writing and editing. Dr. K.M. involved in monitoring, proof reading, final editing, and guidance.

Funding The author(s) reported there is no funding associated with the work featured in this article.

Data availability Not applicable.

Declarations

Conflict of interest The authors declare that they have no known competing financial interests or personal relationships that could have appeared to influence the work reported in this paper.

Ethical approval Not applicable.

Informed consent Not applicable.

Human and animal rights Not applicable.

References

- Harvey AL, Edrada-Ebel R, Quinn RJ (2015) The re-emergence of natural products for drug discovery in the genomics era. *Nat Rev Drug Discov* 14:111–129. <https://doi.org/10.1038/nrd4510>
- Newman DJ, Cragg GM (2020) Natural products as sources of new drugs over the nearly four decades from 01/1981 to 09/2019. *J Nat Prod* 83:770–803. <https://doi.org/10.1021/acs.jnatprod.9b01285>
- Dehelean CA, Marcovici I, Soica C, et al (2021) Plant-derived anticancer compounds as new perspectives in drug discovery and alternative therapy. *Molecules* 26
- Rajan VK, Shameera Ahamed TK, Muraleedharan K (2018) Studies on the UV filtering and radical scavenging capacity of the bitter masking flavanone Eriodictyol. *J Photochem Photobiol B Biol* 185:254–261. <https://doi.org/10.1016/j.jphotobiol.2018.06.017>
- Rajan VK, Muraleedharan K (2017) A computational investigation on the structure, global parameters and antioxidant capacity of a polyphenol, Gallic acid. *Food Chem* 220:93–99. <https://doi.org/10.1016/j.foodchem.2016.09.178>
- Sumayya PC, Mujeeb VMA, Muraleedharan K (2022) Radical scavenging capacity, UV activity, and molecular docking studies of 2', 5', 3, 4-Tetrahydroxychalcone: An insight into the photoprotection. *Chem Phys Impact* 5:100126. <https://doi.org/10.1016/j.chphi.2022.100126>
- Shameera Ahamed TK, Rajan VK, Sabira K, Muraleedharan K (2019) DFT and QTAIM based investigation on the structure and antioxidant behavior of lichen substances Atranorin, Evernic acid and Diffractaic acid. *Comput Biol Chem* 80:66–78. <https://doi.org/10.1016/j.compbiolchem.2019.03.009>
- Ragi C, Muraleedharan K (2023) Antioxidant activity of Hibiscetin and Hibiscitrin: insight from DFT, NCI, and QTAIM. *Theor Chem Acc* 142:30. <https://doi.org/10.1007/s00214-023-02970-5>
- Grzesik M, Naparło K, Bartosz G, Sadowska-Bartosz I (2018) Antioxidant properties of catechins: Comparison with other antioxidants. *Food Chem* 241:480–492. <https://doi.org/10.1016/j.foodchem.2017.08.117>
- Pietta P-G (2000) Flavonoids as Antioxidants. *J Nat Prod* 63:1035–1042. <https://doi.org/10.1021/np9904509>
- Rajan VK, Ragi C, Muraleedharan K (2019) A computational exploration into the structure, antioxidant capacity, toxicity and drug-like activity of the anthocyanidin “Petunidin.” *Heliyon* 5:e02115. <https://doi.org/10.1016/j.heliyon.2019.e02115>
- Rajan VK, Hasna CK, Muraleedharan K (2018) The natural food colorant Peonidin from cranberries as a potential radical scavenger—A DFT based mechanistic analysis. *Food Chem* 262:184–190. <https://doi.org/10.1016/j.foodchem.2018.04.074>
- Pottachola S, Kaniyantavida A, Karuvanthodiyil M (2021) DFT study of structure and radical scavenging activity of natural pigment delphinidin and derivatives. In: Glossman-Mitnik D (ed). *IntechOpen, Rijeka*, p Ch. 16
- Borges Bubols G, da Rocha VD, Medina-Remon A et al (2013) The Antioxidant activity of coumarins and flavonoids. *Mini-Reviews Med Chem* 13:318–334
- Hamadouche S, Ounissi A, Baira K et al (2021) Theoretical evaluation of the antioxidant activity of some stilbenes using the Density Functional Theory. *J Mol Struct* 1229:129496. <https://doi.org/10.1016/j.molstruc.2020.129496>
- Gonzalez-Burgos E, Gomez-Serranillos MP (2012) Terpene compounds in nature: a review of their potential antioxidant activity. *Curr Med Chem* 19:5319–5341
- Perrelli A, Goitre L, Salzano AM et al (2018) Biological activities, health benefits, and therapeutic properties of Avenanthramides: From skin protection to prevention and treatment of cerebrovascular diseases. *Oxid Med Cell Longev* 2018:6015351. <https://doi.org/10.1155/2018/6015351>
- Li X, Zhou L, Yu Y et al (2022) The potential functions and mechanisms of oat on cancer prevention: A review. *J Agric Food Chem* 70:14588–14599. <https://doi.org/10.1021/acs.jafc.2c06518>
- Yu Y, Zhou L, Li X et al (2022) The progress of nomenclature, structure, metabolism, and bioactivities of oat novel phytochemical: Avenanthramides. *J Agric Food Chem* 70:446–457. <https://doi.org/10.1021/acs.jafc.1c05704>
- Peterson DM, Hahn MJ, Emmons CL (2002) Oat Avenanthramides exhibit antioxidant activities in vitro. *Food Chem* 79:473–478. [https://doi.org/10.1016/S0308-8146\(02\)00219-4](https://doi.org/10.1016/S0308-8146(02)00219-4)
- Bratt K, Sunnerheim K, Bryngelsson S et al (2003) Avenanthramides in Oats (*Avena sativa* L.) and structure–antioxidant activity relationships. *J Agric Food Chem* 51:594–600. <https://doi.org/10.1021/jf020544f>
- Fagerlund A, Sunnerheim K, Dimberg LH (2009) Radical-scavenging and antioxidant activity of Avenanthramides. *Food Chem* 113:550–556. <https://doi.org/10.1016/j.foodchem.2008.07.101>
- Zhang T, Shao J, Gao Y et al (2017) Absorption and elimination of oat Avenanthramides in humans after acute consumption of oat cookies. *Oxid Med Cell Longev* 2017:2056705. <https://doi.org/10.1155/2017/2056705>
- Dimberg LH, Theander O, Lingnert H (1993) Avenanthramides—a group of phenolic antioxidants in oats. *Cereal Chem* 70:637–641
- Sumayya PC, Babu G, Muraleedharan K (2021) Quantum chemical investigation of the antiradical property of avenanthramides, oat phenolics. *Heliyon* 7:e06125. <https://doi.org/10.1016/j.heliyon.2021.e06125>
- Xue Y, Teng Y, Chen M et al (2021) Antioxidant activity and mechanism of Avenanthramides: Double H⁺/e⁻ processes and role of the catechol, guaiacyl, and carboxyl groups. *J Agric Food Chem* 69:7178–7189. <https://doi.org/10.1021/acs.jafc.1c01591>
- Purushothaman A, Jishnu Gopal P, Janardanan D (2022) Mechanistic insights on the radical scavenging activity of oat

- avenanthramides. *J Phys Org Chem* 35:e4391. <https://doi.org/10.1002/poc.4391>
28. Pizzino G, Irrera N, Cucinotta M et al (2017) Oxidative stress: Harms and benefits for human health. *Oxid Med Cell Longev* 2017:8416763. <https://doi.org/10.1155/2017/8416763>
29. Sharifi-Rad M, Anil Kumar N V, Zucca P, et al. (2020) Lifestyle, Oxidative Stress, and Antioxidants: Back and Forth in the Pathophysiology of Chronic Diseases. *Front. Physiol.* 11
30. Mellon I (2004) Transcription-coupled DNA repair, overview. In: Lennarz WJ, Lane MBDT-E of BC (eds). Elsevier, New York, pp 204–208
31. Islam BU, Habib S, Ahmad P et al (2015) Pathophysiological role of peroxynitrite induced DNA damage in human diseases: A special focus on Poly(ADP-ribose) Polymerase (PARP). *Indian J Clin Biochem* 30:368–385. <https://doi.org/10.1007/s12291-014-0475-8>
32. M. J. Frisch, G. W. Trucks, H. B. Schlegel, G. E. Scuseria, M. A. Robb, J. R. Cheeseman, G. Scalmani, V. Barone, G. A. Petersson, H. Nakatsuji, X. Li, M. Caricato, A. V. Marenich, J. Bloino, B. G. Janesko, R. Gomperts, B. Mennucci, H. P. Hratchian, J. V. and DJF (2016) *Gaussian 16*, Revision C.01
33. Tomasi J, Mennucci B, Cammi R (2005) Quantum mechanical continuum solvation models. *Chem Rev* 105:2999–3094. <https://doi.org/10.1021/cr9904009>
34. Analyzer AMW, Lu T (2019) Multiwfn. 7:
35. Humphrey W, Dalke A, Schulten K (1996) VMD: Visual molecular dynamics. *J Mol Graph* 14:33–38. [https://doi.org/10.1016/0263-7855\(96\)00018-5](https://doi.org/10.1016/0263-7855(96)00018-5)
36. Zhang J, Lu T (2021) Efficient evaluation of electrostatic potential with computerized optimized code. *Phys Chem Chem Phys* 23:20323–20328. <https://doi.org/10.1039/D1CP02805G>
37. Khlaifia D, Massuyeau F, Ewels C et al (2017) DFT modeling of novel donor-acceptor (D-A) molecules incorporating 3-hexylthiophene (3HT) for Bulk Heterojunction Solar Cells. *ChemistrySelect* 2:10082–10090. <https://doi.org/10.1002/slct.201701481>
38. Zhan C-G, Nichols JA, Dixon DA (2003) Ionization potential, electron affinity, electronegativity, hardness, and electron excitation energy: molecular properties from density functional theory orbital energies. *J Phys Chem A* 107:4184–4195. <https://doi.org/10.1021/jp0225774>
39. Putz MV (2013) Koopmans' analysis of chemical hardness with spectral-like resolution. *Sci World J* 2013:348415. <https://doi.org/10.1155/2013/348415>
40. Parr RG, Zsentyály LV, Liu S (1999) Electrophilicity Index. *J Am Chem Soc* 121:1922–1924. <https://doi.org/10.1021/ja983494x>
41. Chakraborty D, Chattaraj PK (2021) Conceptual density functional theory based electronic structure principles. *Chem Sci* 12:6264–6279. <https://doi.org/10.1039/d0sc07017c>
42. Dutra FR, de Silva C, S, Custodio R (2021) On the accuracy of the direct method to calculate pKa from electronic structure calculations. *J Phys Chem A* 125:65–73. <https://doi.org/10.1021/acs.jpca.0c08283>
43. Kelly CP, Cramer CJ, Truhlar DG (2006) Aqueous solvation free energies of ions and ion–water clusters based on an accurate value for the absolute aqueous solvation free energy of the proton. *J Phys Chem B* 110:16066–16081. <https://doi.org/10.1021/jp063552y>
44. Mittal A, Vashistha VK, Das DK (2023) Free radical scavenging activity of Gallic acid toward various reactive oxygen, nitrogen, and Sulfur species: a DFT approach. *Free Radic Res* 1–10. <https://doi.org/10.1080/10715762.2023.2197556>
45. Coimbra M, Isacchi B, van Bloois L et al (2011) Improving solubility and chemical stability of natural compounds for medicinal use by incorporation into liposomes. *Int J Pharm* 416:433–442. <https://doi.org/10.1016/j.ijpharm.2011.01.056>
46. Abdel-Mottaleb MSA (2016) DFT studies of caffeic acid antioxidant: molecular orbitals and composite reactivity maps correlation with photophysical characteristics and photochemical stability. *J Chem* 2016:8727130. <https://doi.org/10.1155/2016/8727130>
47. Marković Z, Tošović J, Milenković D, Marković S (2016) Revisiting the solvation enthalpies and free energies of the proton and electron in various solvents. *Comput Theor Chem* 1077:11–17. <https://doi.org/10.1016/j.comptc.2015.09.007>
48. Ferreira CA, Ni D, Rosenkrans ZT, Cai W (2018) Scavenging of reactive oxygen and nitrogen species with nanomaterials. *Nano Res* 11:4955–4984. <https://doi.org/10.1007/s12274-018-2092-y>
49. Alfadda AA, Sallam RM (2012) Reactive oxygen species in health and disease. *J Biomed Biotechnol* 2012:936486. <https://doi.org/10.1155/2012/936486>
50. Galano A (2015) Free radicals induced oxidative stress at a molecular level: The current status, challenges and perspectives of computational chemistry based protocols
51. Bartmess JE (1994) Thermodynamics of the Electron and the Proton. *J Phys Chem* 98:6420–6424. <https://doi.org/10.1021/j100076a029>
52. Najafi H (2013) Theoretical study of the substituent effects on the reaction enthalpies of the antioxidant mechanisms of stobadine derivatives in the gas-phase and water. *J Theor Comput Chem* 12:
53. Martínez A, Hernández-Marin E, Galano A (2012) Xanthonas as antioxidants: A theoretical study on the thermodynamics and kinetics of the single electron transfer mechanism. *Food Funct* 3:442–450. <https://doi.org/10.1039/C2FO10229C>
54. Mittal A, Kakkar R (2020) The effect of solvent polarity on the antioxidant potential of echinatin, a retrochalcone, towards various ROS: a DFT thermodynamic study. *Free Radic Res* 54:777–786. <https://doi.org/10.1080/10715762.2020.1849670>

Publisher's Note Springer Nature remains neutral with regard to jurisdictional claims in published maps and institutional affiliations.

Springer Nature or its licensor (e.g. a society or other partner) holds exclusive rights to this article under a publishing agreement with the author(s) or other rightsholder(s); author self-archiving of the accepted manuscript version of this article is solely governed by the terms of such publishing agreement and applicable law.